Accepted Manuscript

A new application for transition metal chalcogenides: WS2 catalysed esterification of carboxylic acids

Vannia C. dos Santos, Lee J. Durndell, Mark A. Isaacs, Christopher M.A. Parlett, Karen Wilson, Adam F. Lee

PII: S1566-7367(16)30447-2
DOI: doi: 10.1016/j.catcom.2016.12.003
Reference: CATCOM 4872

To appear in: *Catalysis Communications*

Received date: 19 September 2016
Revised date: 7 November 2016
Accepted date: 2 December 2016

Please cite this article as: Vannia C. dos Santos, Lee J. Durndell, Mark A. Isaacs, Christopher M.A. Parlett, Karen Wilson, Adam F. Lee , A new application for transition metal chalcogenides: WS2 catalysed esterification of carboxylic acids. The address for the corresponding author was captured as affiliation for all authors. Please check if appropriate. Catcom(2016), doi: 10.1016/j.catcom.2016.12.003

A new application for transition metal chalcogenides: WS_2 catalysed esterification of carboxylic acids

Vannia C. dos Santos[a], Lee J. Durndell[a], Mark A. Isaacs,[a] Christopher M.A. Parlett, Karen Wilson[a] and Adam F. Lee[a]*

[a]*European Bioenergy Research Institute, Aston University, Birmingham B4 7ET, UK.*

Abstract

The first application of WS_2, a well-known graphene analogue, as a solid acid catalyst for carboxylic acid esterification is reported. WS_2 exhibits excellent specific activities and high conversion to methyl esters of (65-90 %) for C2-C16 carboxylic acid esterification with methanol under mild conditions, with Turnover Frequencies between 80-180 h^{-1}, and outstanding water tolerance even under equimolar water spiking. WS_2 also exhibits good stability towards methyl propanoate in the continuous esterification of propanoic acid, and is a promising candidate for biofuels production.

Keywords: Tungsten; Sulfide; Esterification, Carboxylic acid; Biofuels.

Introduction

Transition-metal chalcogenides (TMCs), particularly the group VI transition metal sulfides of W and Mo, have experienced a recent resurgence of academic interest because of their two-dimensional, ordered layered structures, and associated advantageous functional properties [1-3]. Akin to graphene, TMC sulphides are held together by strong intralayer covalent M-S bonds, with weaker Van der Waals interlayer interactions [4]. The resulting anisotropic layered structures offer excellent optical, electronic and mechanical properties, and hence a broad of applications as catalysts, lubricants, photoconductors, sensors, energy storage and medical devices (including drug delivery agents) [2, 4-6]. TMCs have been synthesised in a plethora of tunable morphologies, including nanotubes, nanoplates, nanorods, nanoflowers, nanowires and nanospheres, accompanied by diverse surface physicochemical properties [4, 7-9]. Although TMCs exhibit remarkable thermal and chemical stabilities due to their strong M-S bonding [10], the weak Van der Waals interlayer forces provide opportunities to prepare single and few layer nanosheets. Nanoparticulate and ultrathin TMC materials display unusual physical, chemical and electronic properties, particularly at their edges, compared to bulk analogues due to quantum confinement effects [3].

Band gap engineering offers a route to tune the electronic properties of graphene; TMCs such as WS_2 and MoS_2 are narrow band gap semiconductors whose electronic properties, such as charge transport, ion/small molecule intercalation, catalytic and optical properties, can likewise be tailored [1, 2]. Atomic defects in TMCs can also significantly affect their physical and chemical properties [11], and hence potentially their catalytic performance. Recent time-resolved annular dark-field imaging and spatially resolved electron energy-loss spectroscopy has visualised the formation of single atom S and W defects, including vacancies and edge atoms, in WS_2 nanoribbons [11]. Anion defects will result in under-coordinated W atoms which are expected to behave as classic Lewis acid centres [8]. Vacancy formation could also result in electron delocalisation over W-S-W neighbours, requiring charge compensation by surface protons and hence the generation of Brønsted acidic character [11, 12].

MoS_2 and WS_2 have long been reported as effective hydrotreating catalysts for hydrocracking and hydrodesulfurization in conventional oil refineries [13, 14] due to their low cost and toxicity and excellent thermal and chemical stability. However, there are no reports on their application as solid acid catalysts for sustainable chemical transformations, such as the upgrading of pyrolysis bio-oils through carboxylic acid neutralisation [15] or biodiesel production from free fatty acid components of non-edible plant and algal oils [16-19], in both cases by esterification with short chain alcohols. Here we report the first demonstration of WS_2 for the catalytic esterification of carboxylic acids under mild reaction conditions for applications in the renewable energy sector.

Experimental

N_2 porosimetry was performed on a Quantachrome Nova 4000 porosimeter, with BET surface areas calculated over the range P/P0 = 0.03−0.19, wherein a linear relationship was maintained. X-ray powder diffraction (XRD) on a Bruker D8 Advance diffractometer using the Cu K_α line in the range 2θ = 10−80° with a step size of 0.04°. Acid site loadings were determined by thermogravimetric analysis coupled with mass spectrometry (TGA-MS). Samples were wet-impregnated with propylamine, and then dried in vacuo at 40 °C overnight. TGA was performed on a Mettler Toledo TGA/DSC2 Star system with a heating rate of 10 °C.min^{-1} from 40-800 °C under N_2 flow (30 mL.min^{-1}). Evolved gas analysis was performed with a ThermoStar mass spectrometer connected to the TGA outlet by capillary heated to 180 °C. Ion currents were recorded for the strongest mass fragments of NH_3 (*m/z* 17), unreacted propylamine (*m/z* 30 and 59), and reactively-formed propene (*m/z* 41) and SO_2 (*m/z* 64) formed over acid sites. Ex situ pyridine adsorption was performed by exposure of diluted samples (10 wt % in KBr) to pyridine vapor

overnight. Excess physisorbed pyridine was removed in vacuo at 30 °C prior to recording in vacuo diffuse reflectance infrared Fourier transform (DRIFT) spectra at 50 °C in an environmental cell. Spectra were obtained using a Nicolet Avatar 370 MCT with Smart Collector accessory. Scanning transmission electron microscopy (STEM) was conducted on an aberration corrected JEOL 2100-F electronic microscope operating at 200 kV with samples dispersed on holey carbon grids.

Carboxylic acid esterification with methanol was undertaken using a Radleys Carousel reaction station employing 50 ml glass round-bottomed flasks and magnetic agitation. In a typical experiment, 100 mg of WS_2 nanosheets (Sigma-Aldrich, 99%) was added to a reaction solution of 10 mmol acid and 12.1 ml methanol (alcohol:acid molar ratio = 30:1) pre-heated to 60 °C, from which aliquots were periodically withdrawn for off-line GC analysis on a Shimadzu GC-2010 Plus system with an FID and BP50 30 m x 0.32 mm x 0.25 μm capillary column. Reactions were performed in triplicate, with average values reported. Errors in acid conversion were ±2 %. Re-use experiments were performed for propanoic acid esterification by the addition of an 10 mmol acid

Results and discussion

WS_2 nanosheets (10 $m^2.g^{-1}$) were investigated as a solid acid catalyst for the esterification of methanol and carboxylic acids without pre-activation. The expected layered, two-dimensional structure of WS_2 was confirmed by powder X-ray diffraction (XRD) and high resolution transmission electron microscopy (HRTEM) (Figure 1). XRD patterns of WS_2 were indexed to the 2H (hexagonal stacking arrangement) polymorph of WS2 (JCPDS No. 84-1398). The (002) reflection at 14.3° is characteristic of WS_2 layers stacked along the c axis, with a corresponding interlayer spacing of 0.61 nm, while atomic-resolution images of the (100) surface in Figure 1 reveal a 0.25 nm periodicity consistent with the WS_2 lattice. The N_2 isotherms display reversible type II isotherms, indicative of nonporous materials (Figure S1), with a surprisingly low surface for a microporous material, but which nevertheless consistent with literature values for bulk WS_2 and WS_2 nanotubes of 3-6 $m^2.g^{-1}$ [14, 20]. The solid acidity of WS_2 was probed through NH_3 and propylamine chemisorption and temperature-programmed desorption, in order to quantify their acid loadings and relative strengths. The total acid site density of WS_2 derived by propylamine was 0.21 $mmol.g^{-1}$, comparable to that obtained for sulphated [21] and tungstated [22] zirconias. Reactively-formed propene from propylamine decomposition desorbed between 300-500 °C, and adsorbed ammonia between 200-600 °C, indicative of a mix of medium and strong acid sites (Figure S2). DRIFT spectra of WS_2 following titration with chemisorbed pyridine revealed a 1:1.2 Brønsted:Lewis intensity ratio of the respective bands at 1556 cm^{-1} and 1611 cm^{-1}, indicating mixed acid character (Figure S3). Carboxylic acid esterification is

generally accepted to follow a Brønsted acid catalyzed mechanism involving the formation of a carbenium ion intermediate [23]. As our DRIFT spectra of pyridine titrated WS_2 show, the parent chalcogenide possesses both Brønsted and Lewis acid sites in an approximately equimolar ratio. The latter likely arise from single atom S anion vacancies resulting in under-coordinated W atoms, which are expected to behave as classic Lewis acid centres, however the reaction of such Lewis centres with water and protic reagents [24] can produce Brønsted acid centres during esterification, and the latter are likely the active catalytic sites in this work.

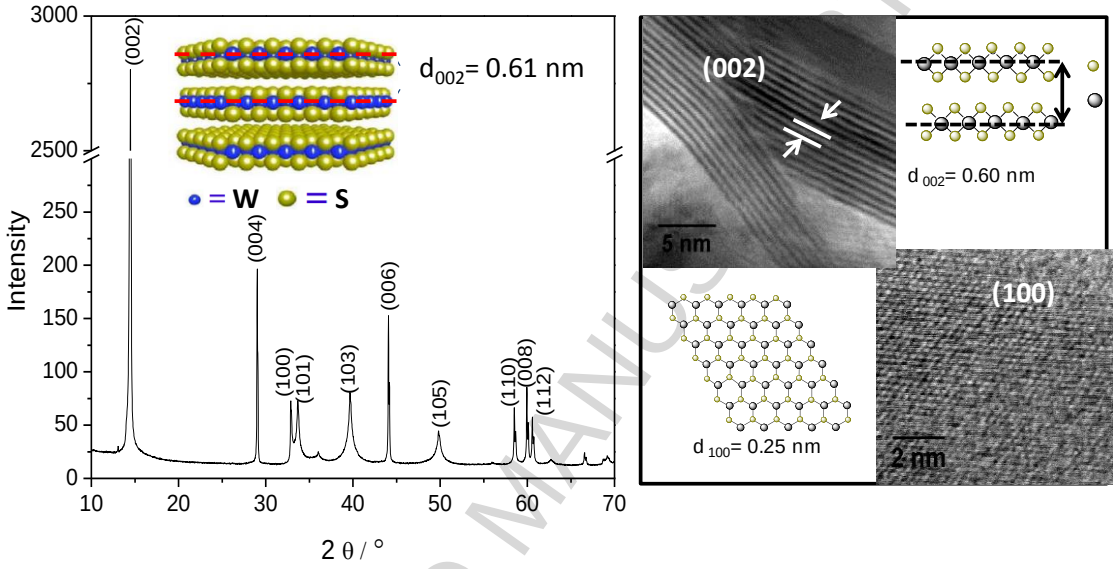

Figure 1. (left) Powder XRD and (right) HRTEM of WS_2 nanosheets highlighting the two-dimensional layers.

The catalytic activity of WS_2 nanosheets was first investigated for carboxylic acid esterification with methanol as a function of acid carbon chain length (Figure 2) in the absence of external mass-transport limitations (Figure S4). A high methanol:acid ratio was deliberately selected to drive the equilibrium esterification to the ester product, and also permits quantitative comparison with other solid acid catalysts employed for carboxylic acid esterification in the literature under the same reaction conditions [15, 22, 25]. High conversions were obtained for a range of C2-C16 carboxylic acids, with even palmitic acid attaining 70 % conversion after 6 h. Resulting activities for C2≈C3 and C6≈C16 for WS_2, indicating that esterification is particularly sensitive to an increase in alkyl chain length between C3 to C6 acids. A similar sharp decrease in the rate of esterification from propanoic to hexanoic acids was previously observed over mesoporous propylsulfonic acid functionalised SBA-15 and KIT-6 [25], and for H_2SO_4 and SAC-13 a silica/Nafion composite [26]. Such decreases are attributed to a combination of polar and steric influences of the alpha substituent on the carboxylic group, with steric and bulk mixing effects dominating for longer chain acids. The interlayer spacing of WS_2 is approximately 0.6 nm

(Figure 1), and hence acid sites within the interlayers will likely be accessible only to acetic and propanoic acids, with hexanoic and palmitic acids only undergoing reaction over the external surface. However, to avoid confusion in the comparison of Turnover Frequencies (TOFs) for short and long chain carboxylic acids, a common approach was adopted in which these were calculated by normalising the initial rate of esterification to the acid site density titrated by propylamine, independent of chain length. This approach will be accurate for the C2 and C3 acids, but underestimate TOFs for C6 and C16 acids. However, this is preferable to the use of a larger basic molecular probe (e.g. t-butylamine) which would only titrate acid sites on the WS_2 external surface, and thereby overestimate TOFs for shorter acids.

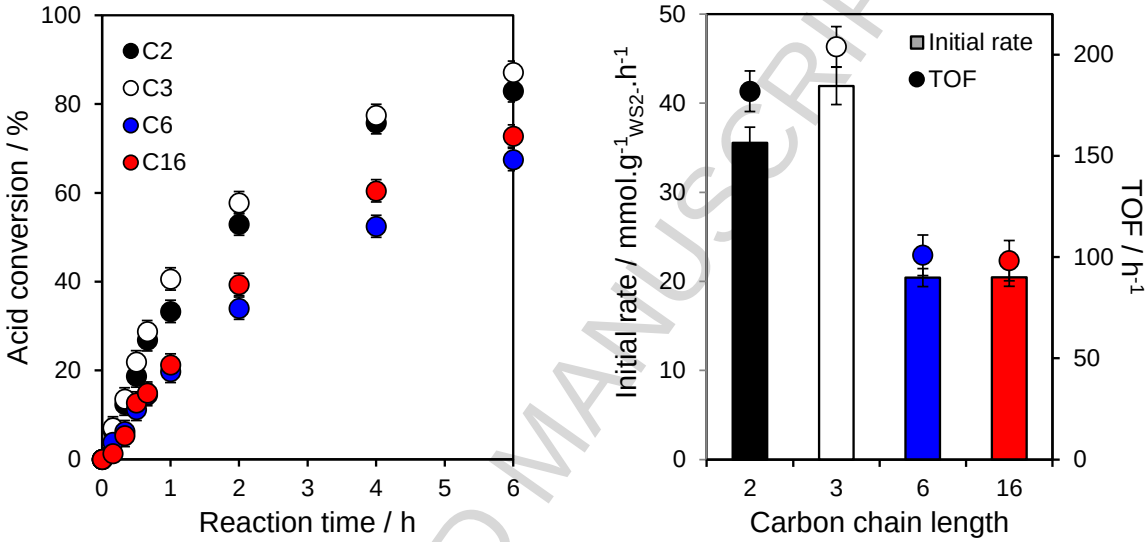

Figure 2. Impact of acid carbon length on carboxylic acid esterification with methanol over WS_2 nanosheets. Reaction conditions: 60 °C, 100 mg catalyst, 10 mmol acid and 12.1 ml methanol (alcohol:acid molar ratio = 30:1).

As noted above, esterification of carboxylic acids is generally accepted to follow a Brønsted acid catalyzed mechanism, and hence it is likely that the active sites in WS_2 are the Brønsted sites observed in Figure S3 by DRIFTS. Mechanistic aspects of acetic acid esterification over heterogeneous Brønsted acid catalysts indicate that the formation of a strongly adsorbed, protonated acid intermediate is followed by rate-limiting step nucleophilic attack by the alcohol to yield a protonated carbonyl through either a single- (Eley-Rideal) [27] or double-site (Langmuir–Hinshelwood) [28, 29] surface reaction. Although initial esterification rates and associated Turnover Frequencies (TOFs) decreased significantly for chain length >C6, TOFs for hexanoic and palmitic acids are almost an order of magnitude higher than those reported for WO_X/ZrO_2 [22] $WO_X/ZrPO_x$ [30], and mesoporous SO_4/ZrO_2 [31], twice those of either sulfonic acid functionalised SBA-15 and KIT-6 mesoporous sílicas [23, 25] or heteropolyacids [32], and only surpassed by homogeneous p-sulfonic acid calix[6]arene and p-hydroxybenzenesulfonic

acid organocatalysts [33], all under comparable reaction conditions (Table 1). WS_2 is hence an exceptional solid acid catalyst for palmitic acid esterification, an important step in the commercial production of biodiesel production from plant oils.

Table 1. Comparative performance of solid acid catalysts for carboxylic acid esterification with methanol.

Catalyst	Carboxylic acid	Temperature / °C	TOF[a]	Ref.
WS_2	Acetic	60	181	-
Propane sulfonic acid[b]	Acetic	50	150	[23]
SO_3H-SBA-15	Acetic	50	120	[23]
WS_2	Hexanoic	60	101	-
SAC-13	Hexanoic	60	130	[26]
$PrSO_3H$-KIT-6-120	Hexanoic	60	72	[25]
WS_2	Palmitic	60	98	-
SO_4/ZrO_2	Palmitic	60	7	[31]
WO_X/ZrO_2	Palmitic	60	9.5	[22]
$WO_X/ZrPO_x$	Palmitic	60	22	[30]
$PrSO_3H$-KIT-6-120	Palmitic	60	51	[30]
IFMC-200	Palmitic	65	13.9	[32]
p-Sulfonic acid calix[6]arene[b]	Palmitic	60	313	[33]
p-Hydroxybenzenesulfonic acid[b]	Palmitic	60	288	[33]

[a]Initial rate normalised per acid site. [b]Homogeneous acid.

Water is an inevitable by-product of esterification, but a common problem for many solid acid catalysts [15, 27, 34], as observed for e.g. acrylic acid esterification with butanol over $Cs_{2.5}H_{0.5}PW_{12}O_{40}$, SO_2^{4-}/ZrO_2, Amberlyst-15, Nafion-H and $H_3PW_{12}O_{40}$, whether through leaching of the active phase, strong adsorption over hydrophilic catalysts, and/or promotion of the reverse ester hydrolysis reaction and displacement of the reaction equilibrium towards the acid. The water tolerance of WS_2 was therefore explored for propionic acid esterification with methanol (Figure 3). Addition of 1 mmol of water (10 mol% equivalent to the acid) had little effect on the initial rate, which fell by around 25 %, whereas high water concentrations (100 mol%) resulted in a 50 % activity loss. While obviously undesirable, this water tolerance remains superior to that observed for acid esterification catalysed by $H_3PW_{12}O_{40}$ functionalised magnetic nanoparticles (for which only 1 wt% water induced 90 % deactivation) [35], SO_4/ZrO_2 [34], Amberlyst-15 [36], and SAC-13 [27] as shown in Table 2. For hydrophilic solid acid catalysts it is strongly believed that deactivation occurs due to irreversible water adsorption over the active sites coupled with a shift in equilibrium position to favour ester hydrolysis. Hence some WS_2 acid sites retain activity even in the presence of extremely high water concentrations.

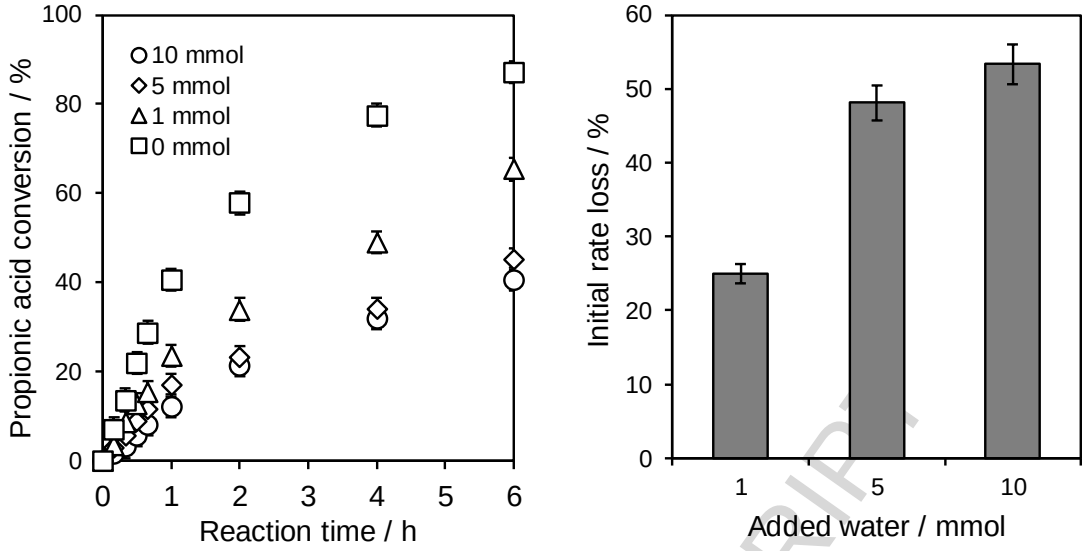

Figure 3. Impact of water on propionic acid esterification with methanol over WS_2 nanosheets. Reaction conditions: 60 °C, 100 mg catalyst, 10 mmol acid and 12.1 ml methanol (alcohol:acid molar ratio = 30:1).

Table 2. Comparative water tolerance of solid acid catalysts for carboxylic acid esterification with methanol.

Catalyst	Carboxylic acid	Water content relative to carboxylic acid / mol%	Deactivation[a] / %	Ref.
WS_2	Propionic	100	53	-
SAC-13	Acetic	95	60	[27]
Amberlyst-15	Acrylic	100	70	[34]
Nafion-H	Acrylic	100	49	[34]
SO_4/ZrO_2	Acrylic	100	100	[34]
Amberlyst-15	Oleic	20	21	[36]
SiO_2-MNP-1-HPA	Palmitic	28	90	[35]

[a]Relative loss of conversion or initial rate following water addition.

WS_2 also demonstrated excellent re-usability, delivering >90 % propanoic acid esterification over three consecutive reactions (Figure 4), and proved amenable to continuous esterification in a plug-flow reactor wherein constant methyl propanoate ester productivity was observed over 6 h (Figure S5). While conversion was obviously lower in the latter case due to the shorter contact time with the catalyst, plug-flow operation permits continuous ester production with integrated product separation.

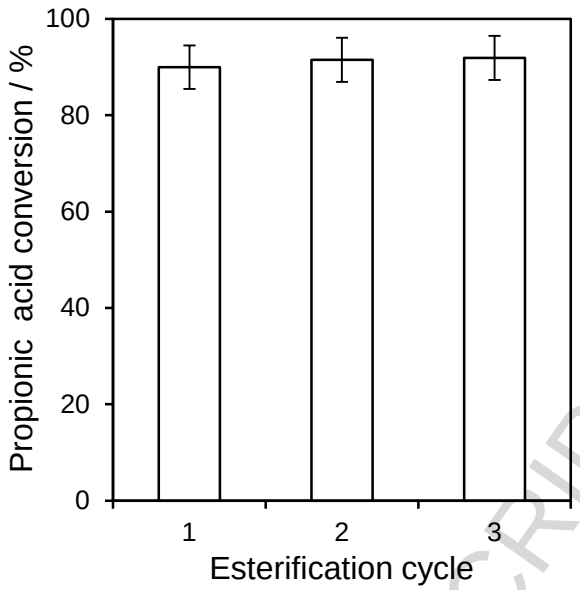

Figure 4. Recyclability of WS_2 nanosheets for propanoic acid esterification with methanol. Reaction conditions: 60 °C, 100 mg catalyst, 10 mmol acid and 12.1 ml methanol; an additional 10 mmol acid was added after each 6 h reaction.

Conclusions

A new application for WS_2 is demonstrated, as a solid acid catalyst demonstrating excellent catalytic activity for esterification reactions under relatively mild conditions. We believe this to be the first example of WS_2 investigated for use in this particular application. Activity was maintained in C6 and C16 acid esterification, suggesting WS_2 analogues could find potential use in bio-oil upgrading and biodiesel production from free fatty acids. We believe that tuneable morphologies (nanostructures) or the preparation of a stable, single layer structure could further improve catalytic activity, with respect to the current WS_2 nanosheets, for any reaction that follows an acid site mechanism. WS_2 appears as an excellent, low cost and robust material demonstrating highly active acidic species for acid esterification.

Acknowledgments

We thank the EPSRC (EP/K000616/2 and EP/K014749/1) for financial support. Support from the European Union Seventh Framework Programme (FP7/2007-2013) under grant agreement no. 604307 is also acknowledged. VCS acknowledges CNPq (Conselho Nacional de Desenvolvimento Cientifico e Tecnológico) for the award of a postdoctoral scholarship. We acknowledge the Nanoscale Physics Group at the University of Birmingham for HRTEM access.

References

[1] M. Chhowalla, H.S. Shin, G. Eda, L.-J. Li, K.P. Loh, H. Zhang, The chemistry of two-dimensional layered transition metal dichalcogenide nanosheets, Nat Chem, 5 (2013) 263-275.
[2] C. Tan, H. Zhang, Two-dimensional transition metal dichalcogenide nanosheet-based composites, Chemical Society Reviews, 44 (2015) 2713-2731.
[3] R. Lv, J.A. Robinson, R.E. Schaak, D. Sun, Y. Sun, T.E. Mallouk, M. Terrones, Transition Metal Dichalcogenides and Beyond: Synthesis, Properties, and Applications of Single- and Few-Layer Nanosheets, Accounts of Chemical Research, 48 (2015) 56-64.
[4] A.R. Adini, M. Redlich, R. Tenne, Medical applications of inorganic fullerene-like nanoparticles, Journal of Materials Chemistry, 21 (2011) 15121-15131.
[5] H. Liu, D. Su, G. Wang, S.Z. Qiao, An ordered mesoporous WS2 anode material with superior electrochemical performance for lithium ion batteries, Journal of Materials Chemistry, 22 (2012) 17437-17440.
[6] L. Cheng, W. Huang, Q. Gong, C. Liu, Z. Liu, Y. Li, H. Dai, Ultrathin WS2 Nanoflakes as a High-Performance Electrocatalyst for the Hydrogen Evolution Reaction, Angewandte Chemie International Edition, 53 (2014) 7860-7863.
[7] L. Rapoport, Y. Bilik, Y. Feldman, M. Homyonfer, S.R. Cohen, R. Tenne, Hollow nanoparticles of WS2 as potential solid-state lubricants, Nature, 387 (1997) 791-793.
[8] D.M. Sim, M. Kim, S. Yim, M.-J. Choi, J. Choi, S. Yoo, Y.S. Jung, Controlled Doping of Vacancy-Containing Few-Layer MoS2 via Highly Stable Thiol-Based Molecular Chemisorption, ACS Nano, 9 (2015) 12115-12123.
[9] H. Wang, H. Yuan, S. Sae Hong, Y. Li, Y. Cui, Physical and chemical tuning of two-dimensional transition metal dichalcogenides, Chemical Society Reviews, 44 (2015) 2664-2680.
[10] C. Schuffenhauer, G. Wildermuth, J. Felsche, R. Tenne, How stable are inorganic fullerene-like particles? Thermal analysis (STA) of inorganic fullerene-like NbS2, MoS2, and WS2 in oxidizing and inert atmospheres in comparison with the bulk material, Physical Chemistry Chemical Physics, 6 (2004) 3991-4002.
[11] Z. Liu, K. Suenaga, Z. Wang, Z. Shi, E. Okunishi, S. Iijima, Identification of active atomic defects in a monolayered tungsten disulphide nanoribbon, Nat Commun, 2 (2011) 213.
[12] Y.-C. Lin, T. Björkman, H.-P. Komsa, P.-Y. Teng, C.-H. Yeh, F.-S. Huang, K.-H. Lin, J. Jadczak, Y.-S. Huang, P.-W. Chiu, A.V. Krasheninnikov, K. Suenaga, Three-fold rotational defects in two-dimensional transition metal dichalcogenides, Nat Commun, 6 (2015).
[13] R.R. Chianelli, M.H. Siadati, M.P. De la Rosa, G. Berhault, J.P. Wilcoxon, R. Bearden, B.L. Abrams, Catalytic Properties of Single Layers of Transition Metal Sulfide Catalytic Materials, Catalysis Reviews, 48 (2006) 1-41.
[14] Y.G. Hur, M.-S. Kim, D.-W. Lee, S. Kim, H.-J. Eom, G. Jeong, M.-H. No, N.S. Nho, K.-Y. Lee, Hydrocracking of vacuum residue into lighter fuel oils using nanosheet-structured WS2 catalyst, Fuel, 137 (2014) 237-244.
[15] J.C. Manayil, C.V.M. Inocencio, A.F. Lee, K. Wilson, Mesoporous sulfonic acid silicas for pyrolysis bio-oil upgrading via acetic acid esterification, Green Chemistry, 18 (2016) 1387-1394.
[16] A.A. Kiss, A.C. Dimian, G. Rothenberg, Solid Acid Catalysts for Biodiesel Production –- Towards Sustainable Energy, Advanced Synthesis & Catalysis, 348 (2006) 75-81.
[17] A.F. Lee, J.A. Bennett, J.C. Manayil, K. Wilson, Heterogeneous catalysis for sustainable biodiesel production via esterification and transesterification, Chemical Society Reviews, 43 (2014) 7887-7916.
[18] F. Su, Y. Guo, Advancements in solid acid catalysts for biodiesel production, Green Chemistry, 16 (2014) 2934-2957.
[19] J.A. Melero, L.F. Bautista, J. Iglesias, G. Morales, R. Sánchez-Vázquez, K. Wilson, A.F. Lee, New insights in the deactivation of sulfonic modified SBA-15 catalysts for biodiesel production from low-grade oleaginous feedstock, Applied Catalysis A: General, 488 (2014) 111-118.

[20] M. Grilc, G. Veryasov, B. Likozar, A. Jesih, J. Levec, Hydrodeoxygenation of solvolysed lignocellulosic biomass by unsupported MoS2, MoO2, Mo2C and WS2 catalysts, Applied Catalysis B: Environmental, 163 (2015) 467-477.
[21] G. Morales, A. Osatiashtiani, B. Hernandez, J. Iglesias, J.A. Melero, M. Paniagua, D. Robert Brown, M. Granollers, A.F. Lee, K. Wilson, Conformal sulfated zirconia monolayer catalysts for the one-pot synthesis of ethyl levulinate from glucose, Chemical Communications, 50 (2014) 11742-11745.
[22] V.C. dos Santos, K. Wilson, A.F. Lee, S. Nakagaki, Physicochemical properties of WOx/ZrO2 catalysts for palmitic acid esterification, Applied Catalysis B: Environmental, 162 (2015) 75-84.
[23] S. Miao, B.H. Shanks, Mechanism of acetic acid esterification over sulfonic acid-functionalized mesoporous silica, Journal of Catalysis, 279 (2011) 136-143.
[24] M. Hino, M. Kurashige, H. Matsuhashi, K. Arata, The surface structure of sulfated zirconia: Studies of XPS and thermal analysis, Thermochimica Acta, 441 (2006) 35-41.
[25] C. Pirez, J.-M. Caderon, J.-P. Dacquin, A.F. Lee, K. Wilson, Tunable KIT-6 Mesoporous Sulfonic Acid Catalysts for Fatty Acid Esterification, ACS Catalysis, 2 (2012) 1607-1614.
[26] Y. Liu, E. Lotero, J.G. Goodwin Jr, Effect of carbon chain length on esterification of carboxylic acids with methanol using acid catalysis, Journal of Catalysis, 243 (2006) 221-228.
[27] Y. Liu, E. Lotero, J.G. Goodwin Jr, A comparison of the esterification of acetic acid with methanol using heterogeneous versus homogeneous acid catalysis, Journal of Catalysis, 242 (2006) 278-286.
[28] A. Corma, H. Garcia, S. Iborra, J. Primo, Modified faujasite zeolites as catalysts in organic reactions: Esterification of carboxylic acids in the presence of HY zeolites, Journal of Catalysis, 120 (1989) 78-87.
[29] H.T.R. Teo, B. Saha, Heterogeneous catalysed esterification of acetic acid with isoamyl alcohol: kinetic studies, Journal of Catalysis, 228 (2004) 174-182.
[30] K.N. Rao, A. Sridhar, A.F. Lee, S.J. Tavener, N.A. Young, K. Wilson, Zirconium phosphate supported tungsten oxide solid acid catalysts for the esterification of palmitic acid, Green Chemistry, 8 (2006) 790-797.
[31] K. Saravanan, B. Tyagi, R.S. Shukla, H.C. Bajaj, Esterification of palmitic acid with methanol over template-assisted mesoporous sulfated zirconia solid acid catalyst, Applied Catalysis B: Environmental, 172–173 (2015) 108-115.
[32] D.-Y. Du, J.-S. Qin, Z. Sun, L.-K. Yan, M. O'Keeffe, Z.-M. Su, S.-L. Li, X.-H. Wang, X.-L. Wang, Y.-Q. Lan, An unprecedented (3,4,24)-connected heteropolyoxozincate organic framework as heterogeneous crystalline Lewis acid catalyst for biodiesel production, Scientific Reports, 3 (2013) 2616.
[33] R. Natalino, E.V.V. Varejao, M.J. da Silva, A.L. Cardoso, S.A. Fernandes, p-Sulfonic acid calix[n]arenes: the most active and water tolerant organocatalysts in esterification reactions, Catalysis Science & Technology, 4 (2014) 1369-1375.
[34] X. Chen, Z. Xu, T. Okuhara, Liquid phase esterification of acrylic acid with 1-butanol catalyzed by solid acid catalysts, Applied Catalysis A: General, 180 (1999) 261-269.
[35] X. Duan, Y. Liu, Q. Zhao, X. Wang, S. Li, Water-tolerant heteropolyacid on magnetic nanoparticles as efficient catalysts for esterification of free fatty acid, RSC Advances, 3 (2013) 13748-13755.
[36] J.-Y. Park, Z.-M. Wang, D.-K. Kim, J.-S. Lee, Effects of water on the esterification of free fatty acids by acid catalysts, Renewable Energy, 35 (2010) 614-618.

Graphical abstract

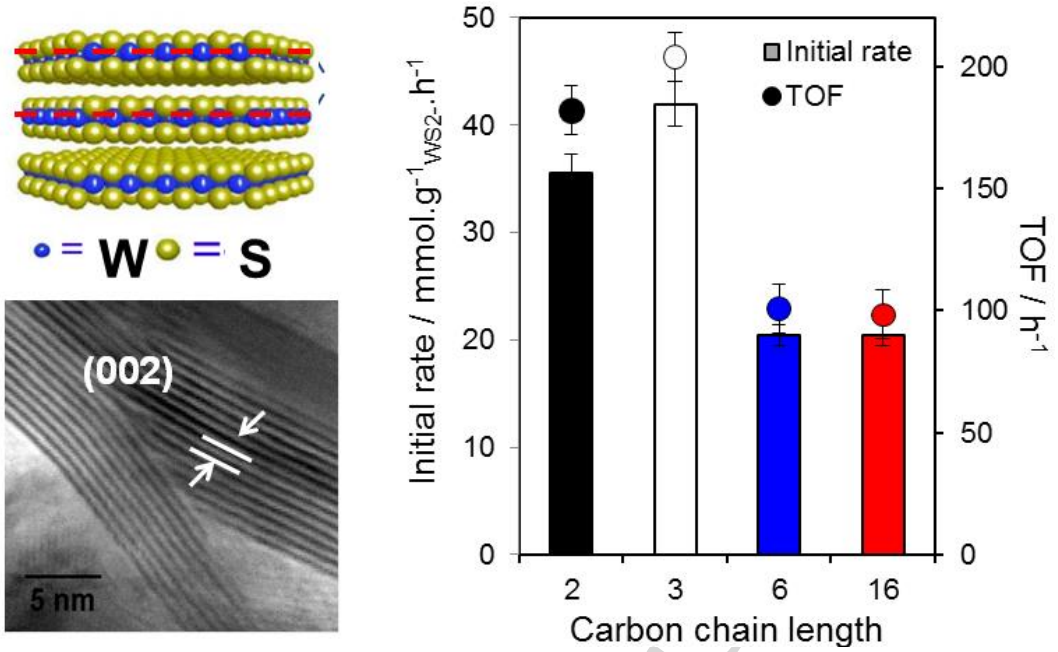

Highlights

- WS_2 is a promising active solid acid catalyst for carboxylic acid esterification
- Highest reported TOFs for C2-C16 free fatty acids by a heterogeneous catalyst
- Excellent water tolerance and stability
- Continuous production of methyl propanoate ester demonstrated in plug-flow